

Different Topologies of DC/DC Converter Used in PV Systems with MPPT Controllers Based on Perturb and Observe Algorithm and Sliding Mode Theory

Radhia Garraoui

Photovoltaic, Wind and Geothermal Systems Research Unit, National Engineering School of Gabes, TUNISIA
Email: radhiagarraoui@gmail.com

Mouna Ben Hamed

Photovoltaic, Wind and Geothermal Systems Research Unit, National Engineering School of Gabes, TUNISIA
Email: mouna.benhamed@enig.rnu.tn

Lassaad Sbita

Photovoltaic, Wind and Geothermal Systems Research Unit, National Engineering School of Gabes, TUNISIA
Email: lassaad.sbita@enig.rnu.tn

Abstract—In this paper two algorithms of maximum power point tracking controller applied for photovoltaic power generation systems are presented, one classical and the other one is based on the principle of the sliding mode theory. A comparative study between the two controllers is applied to the photovoltaic system using different topologies of DC/DC converters based on boost, SEPIC and Ćuk converters.

The performance comparison between the two controllers has been carried out to demonstrate the effectiveness of MPPT controller based on the principle of sliding mode theory against change in working conditions. Matlab/simulation results show that both techniques give improved performance in a transient state, steady state and sliding controller gives better efficiency compared with PandO. In this work the SEPIC converter shows better operation than the boost and the Ćuk converter.

Index Terms—Perturb and observe controller, sliding mode approach, photovoltaic system, Boost converter, SEPIC converter, Ćuk converter.

I INTRODUCTION

The future global economy is likely to consume ever more energy, especially with the rising energy demand of developing countries [1]. We rely on coal, oil and gas (the fossil fuels) for over 80% of our current energy needs this energy demand is expected to grow by almost half over the next two decades. This energy demand is expected to grow by almost half over the next two decades. We need to look at both the short-term and long-term to help reduce carbon emissions, we already have many technologies at our disposal: from wind, wave, solar and biomass for heat and power. Solar technology is at the heart of the renewable energy [2] and has been a key source of new electricity generation for the last few years. The photovoltaic characteristic is nonlinear and changes with irradiation and temperature. In general, there

is a point on the voltage-current or voltage-power curves, called the maximum power point (MPP), where PV panel operates with maximum efficiency and produces its maximum output power. The state of the art techniques to track the maximum available output power of PV systems are called the maximum-power point tracking (MPPT). Controlling MPPT for the solar array is essential in a PV system. There are many techniques have been developed to implement MPPT, these techniques are different in their efficiency, speed, hardware implementation, cost, popularity [3, 4]. One of the most widely used techniques in MPPT is PandO due to its simple and easily implementation [5]. Switch Mode Power Supply topologies follow a set of rules. A very large number of converters have been proposed, which however can be seen to be minor variations of a group of basic DC/DC converters built on a set of rules [6]. Many consider the basic group to consist of the three: Buck, Boost and Buck-Boost converters. The Ćuk, essentially a Boost-Buck converter, may not be considered as basic converter along with its variations: the SEPIC and the zeta converters. In this paper a comparison between three types of converters the boost, the SEPIC and the Ćuk is presented. Also, a control technique using the principle of sliding theory is associated with an MPPT controller in order to improve energy conversion efficiency and compared with PandO method. The difference between the three converters topologies is also presented via simulation work.

II MODELING AND CHARACTERISTIC OF SOLAR PANEL

The model of solar cell can be categorized as p-n semiconductor junction, when exposed to light, the current is

generated. The PV cell equivalent circuit can be represented as an ideal current source, diode, parallel resistance and a series resistance as shown in Fig.1, where the current source is the light generated current which is directly proportional to the solar irradiation. The series and the shunt resistances represent a voltage loss on the way to the external contacts and the leakage current in the shunt path respectively [7, 8].

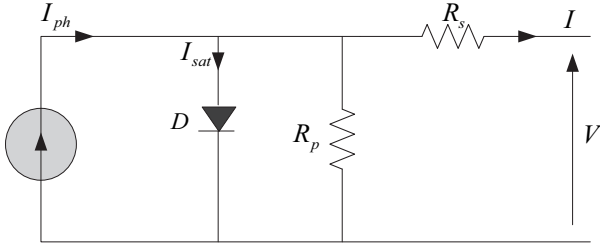


Fig. 1: Equivalent model of a solar cell.

Equation (1) describes the output current of the cell:

$$I = I_{ph} - I_{sat} \left[e^{\left(\frac{q}{k} K_b T A V\right)} - 1 \right] \quad (1)$$

The generated photocurrent I_{ph} is given as:

$$I_{ph} = \frac{G}{G_r} [I_{scr} + K_i (T - T_r)] \quad (2)$$

The diode saturation current is given by:

$$I_{sat} = I_{rr} \left[\frac{T}{T_r} \right]^3 e^{\left[\frac{q E_g}{K_b A} \left(\frac{1}{T_r} - \frac{1}{T} \right) \right]} \quad (3)$$

It is clear from Fig.2, and Fig.3 that the PV module has a nonlinear P-V characteristic which differs according to solar irradiation and temperature. Each curve has a different point at which the module can produce its maximum power. Hence, in order to overcome this problem, an MPPT controller is required.

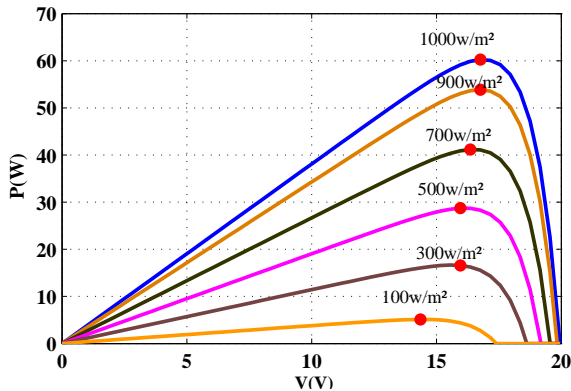


Fig. 2: P-V characteristic under different irradiation values and constant temperature $T=25^\circ\text{C}$.

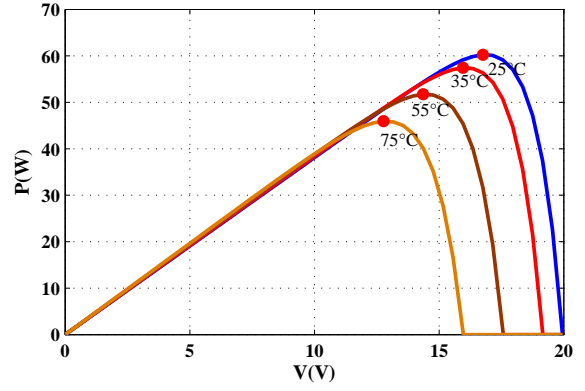


Fig. 3: P-V characteristics under different temperature and constant irradiation $G=1000\text{W}/\text{m}^2$.

III MODELING THE DIFFERENT DC/DC CONVERTERS

A static converter is a meshed network of electrical components that acts as a linking, adapting or transforming stage between two sources, generally between a generator and a load. we present respectively the Circuit schematic of a BOOST converter, a SEPIC converter and a CúK converter with their average models.

III-A Modeling the BOOST converter

The electronic circuit of the Boost converter, also known as the up converter, is shown in Fig.4.

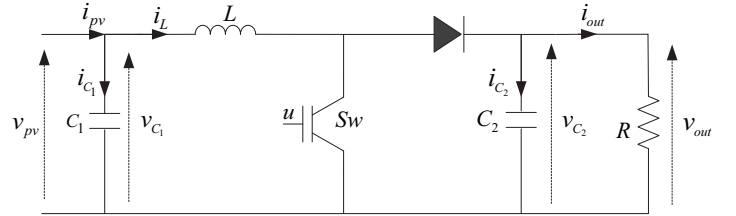


Fig. 4: Equivalent model of a BOOST converter.

To obtain the dynamics of the Boost converter, we may apply Kirchoff's laws in each one of the circuit topologies arising as a consequence of the two switch positions. The first circuit topology is obtained when the switch position function is set to adopt the numerical value "1", and the second circuit topology is obtained when the switch position function takes the value "0".

$$\begin{cases} \frac{\partial i_L}{\partial t} = \frac{1}{L}(v_{C_1} + (u - 1)v_{out}) \\ \frac{\partial v_{C_2}}{\partial t} = \frac{1}{C_2}(i_L(1 - u) - \frac{v_{out}}{R}) \end{cases} \quad (4)$$

III-B Modeling the SEPIC converter

Fig.5 shows the SEPIC DC-to-DC converter circuit with switches realized by means of semiconductor devices (Sw)

and diode D). These operate in a complementary fashion, i.e., when the transistor Sw is in the conducting mode, then the diode D is inversely polarized and vice versa.

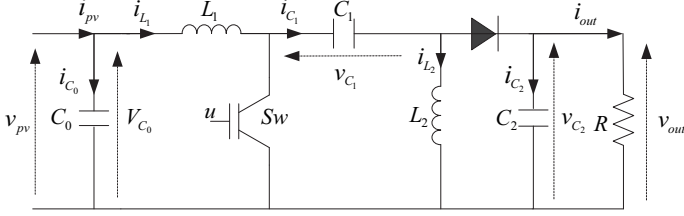


Fig. 5: Equivalent model of SEPIC converter.

The model of the converter is derived to be:

$$\begin{cases} \frac{\partial i_{L1}}{\partial t} = \frac{1}{L_1}((u-1)(v_{C1} + v_{C2}) + v_{C0}) \\ \frac{\partial v_{C1}}{\partial t} = \frac{1}{C_1}(i_{L1}(1-u) - u i_{L2}) \\ \frac{\partial i_{L2}}{\partial t} = \frac{1}{L_2} \cdot (u \cdot v_{C1} - (1-u)v_{C2}) \\ \frac{\partial v_{C2}}{\partial t} = \frac{1}{C_2}((i_{L1} + i_{L2}) \cdot (1-u) - \frac{v_{C2}}{R}) \end{cases} \quad (5)$$

III-C Modeling the Cúk converter

A typical example is the cascade connection of the Boost and the Buck converter which produces the well known Cúk converter. This converter is shown in Fig.6

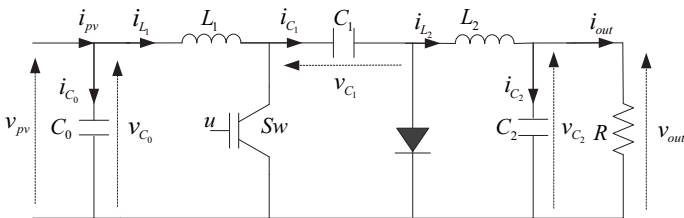


Fig. 6: Equivalent model of Cúk converter.

The Cúk converter dynamics is then described by:

$$\begin{cases} \frac{\partial i_{L1}}{\partial t} = \frac{1}{L_1}((u-1)v_{C1} + v_{C0}) \\ \frac{\partial v_{C1}}{\partial t} = \frac{1}{C_1}(i_{L1}(1-u) + u \cdot i_{L2}) \\ \frac{\partial i_{L2}}{\partial t} = \frac{1}{L_2}(-u \cdot v_{C1} - v_{C2}) \\ \frac{\partial v_{C2}}{\partial t} = \frac{1}{C_2}(i_{L2} - \frac{v_{C2}}{R}) \end{cases} \quad (6)$$

we consider d the duty cycle of the switching control u . H1, H2 and H3 are input voltage and output voltage conversion ratio respectively for BOOST, SEPIC and Cúk converters as illustrated in TABLE.I:

BOOST converter	SEPIC converter	Cúk converter
$H1 = \frac{1}{1-d}$	$H2 = \frac{d}{1-d}$	$H3 = \frac{-d}{1-d}$

TABLE I: Different input voltage and output voltage conversion ratio

Fig.7 shows that for the Step-up (Boost) converter the output voltage is higher than the input voltage, but in the case of SEPIC converter the output voltage can be lower or higher than the input voltage, the Cúk converter allows bidirectional voltage conversion with the output voltage of inverted polarity.

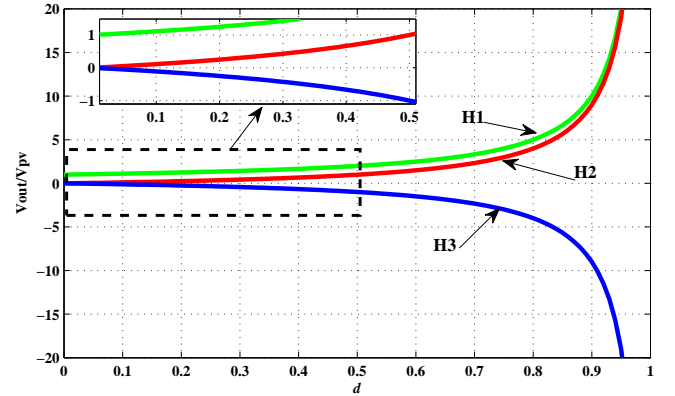


Fig. 7: Different input voltage and output voltage conversion ratio.

IV TECHNIQUES OF MAXIMUM POWER POINT TRACKING

IV-A MPPT based on the principle of the sliding mode theory

The first theoretical work on sliding regimes emerged in the early 60s. Sliding Mode Control is known to be a robust control method appropriate for controlling switched systems. High robustness are maintained against various kinds of uncertainties such as external disturbances and measurement error [9,10].

Generating a sliding regime can be summarized in two steps : the first step is the determination of the sliding surface $S = 0$. The second step allows finding a discontinuous signal input which leads the system trajectories to $S = 0$, from any initial condition. Define the sliding mode $S(t)$ as follows:

$$S(t) = \{x \setminus S(x, t) = 0\}$$

we try to use the principle of the sliding theory to make an MPPT controller For the photovoltaic system, the switching surface will be selected as:

$$\frac{\partial P_{pv}}{\partial I_{pv}} = I_{pv} \left(\frac{\partial V_{pv}}{\partial I_{pv}} + \frac{V_{pv}}{I_{pv}} \right) = 0 \quad (7)$$

This switching surface is here presenting the MPP under certain condition, the nontrivial solution of (7) is:

$$\left(\frac{\partial V_{pv}}{\partial I_{pv}} + \frac{V_{pv}}{I_{pv}} \right) = 0 \quad (8)$$

Thus, in the state space, a proper sliding manifold can be determined through:

$$S(t, x) = \frac{\partial V_{pv}}{\partial I_{pv}} + \frac{V_{pv}}{I_{pv}} \quad (9)$$

This surface expounds the rule for proper switching. When the trajectory state is away from the corresponding surface, a control law tries to return it and maintains its movement around the selected switching surface. The most important and serious mission is to conceive a control law that will drive the trajectory state to the sliding surface and maintain it on the surface this is the second step. To constrain the trajectories of the PV system we propose a control based on sliding mode theory to reach the performances and then, to stay onto the sliding surface Chosen according to the control objectives, the control law is presented in this form :

$$d = d_{eq} + d_{dis} \quad (10)$$

d_{eq} is called equivalent control. Note that, under the action of the equivalent control d_{eq} any trajectory starting from the manifold $S(x) = 0$ remains on it, since $\dot{S}(x) = 0$.

d_{eq} is given by

$$S(t, x) = \dot{S}(t, x) = 0 \quad (11)$$

This ensures the invariance of the sliding surface. The proposed discontinuous control, d_{dis} guarantees a convergence in finite time on the surface; it is defined as:

$$d_{dis} = M \cdot \text{Sign}(S) \quad (12)$$

$$d = \left\{ \begin{array}{l} 1 \\ d_{eq} + M \cdot \text{Sign}(S) \\ 0 \end{array} \right. , \text{if } \left\{ \begin{array}{l} d_{eq} + M \cdot \text{Sign}(S) \geq 1 \\ 0 < d_{eq} + M \cdot \text{Sign}(S) < 1 \\ d_{eq} + M \cdot \text{Sign}(S) \leq 0 \end{array} \right. \quad (13)$$

IV-B MPPT based on the PandO algorithm

The PandO algorithm involves a perturbation in the operating voltage of the DC link between the PV array and the power converter [11]. In this method, the sign of the last perturbation and the sign of the last increment in the power are used to decide what the next perturbation should be.

As can be seen in the scheme of the algorithm shown in Fig.8, on the left of the MPP increasing the voltage increases the power whereas on the right decreasing the voltage increases the power. If there is an increment in the power, the perturbation should be kept in the same direction and if the power decreases, then the next perturbation should be in the opposite direction. Based on these facts, the algorithm is implemented. The process is repeated until the MPP is reached. Then the operating point oscillates around the MPP.

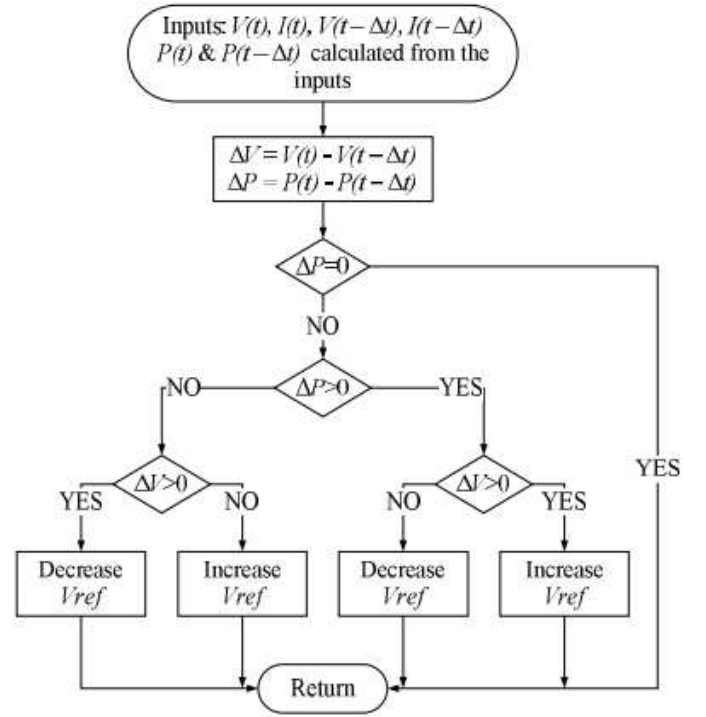


Fig. 8: The scheme of the PandO algorithm.

V SIMULATION RESULTS

An extensive simulation for both techniques has been done using MATLAB and some selected results are presented with a comparison between the MPPT controllers based on sliding theory and PandO algorithm.

We suppose that the irradiations trajectory takes this form: it increases irradiation from $500 \text{ (W/m}^2\text{)}$ to $1000 \text{ (W/m}^2\text{)}$ at $t=0.06 \text{ s}$. This illumination change is applied to the three different converters using every time one of the two MPPT controllers, we start by using the MPPT controller based on the sliding theory, we called it SMC. Fig.9 presents the power response under the irradiation change, the simulation results show that both systems with BOOST converter, *CuK* converter and with SEPIC converter succeed to track the maximum power, it is the same thing in case we use the PandO controller as mentioned in Fig.11, but, both Fig.9 and Fig.11 shows that the MPPT controller based on sliding theory and PandO algorithm with BOOST converter track the maximum power point very fast compared to the system with SEPIC and *CuK* converter. Moreover, the output power from the system with *CuK* converter is not stable at maximum power as compared to the system with BOOST and SEPIC converter, also, the SEPIC is more stable with less power ripple as compared to two other converters at maximum power output.

If we concentrate on the MPPT controllers, we could easily note the good performances of the SMC against the PandO that shows some oscillations but a rapid track of MPP. Fig.10 and Fig.12 shows the waveforms of output voltage, again the PV system with SEPIC shows a performing and precise response but with the BOOST is occurring the most rapid response, the *CuK* converter is producing a negative output voltage.

The load variation allows testing the robustness of the two controllers against parametric changes. The load is changed from 50Ω to 100Ω . As SEPIC converter shows good operation we choose to make test of load variation using it with the two MPPT controllers. Fig.13 and Fig.14 shows that the two controllers resists with success to the parametric changes and guarantees a stable optimal power and precise output voltage for the SMC however the Pand occurs the oscillations as usual, so, from this study we could say that the MPPT controller based on sliding mode theory is more performant that the classical PandO controller and that the SEPIC converter is the most performing

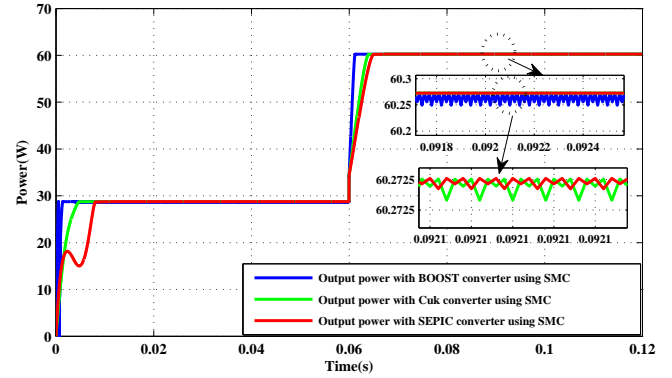


Fig. 9: Output power under variable irradiation using MPPT controller based on sliding theory.

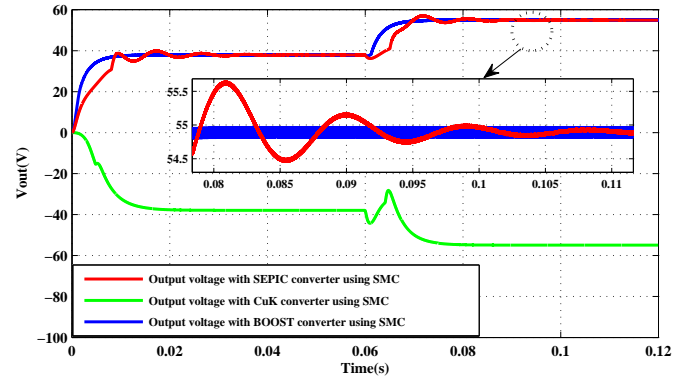


Fig. 10: Output voltage under variable irradiation using MPPT controller based on sliding theory.

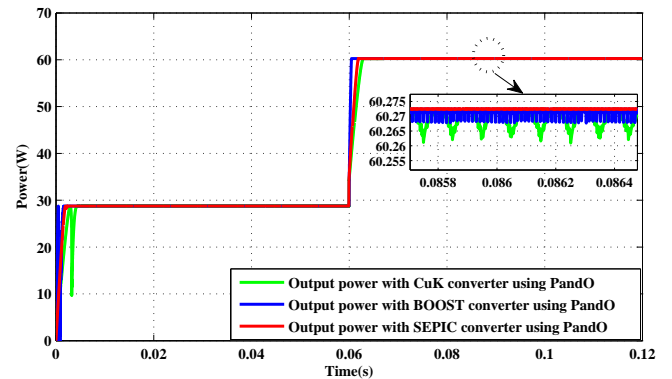


Fig. 11: Output power under variable irradiation using MPPT controller based on PandO algorithm.

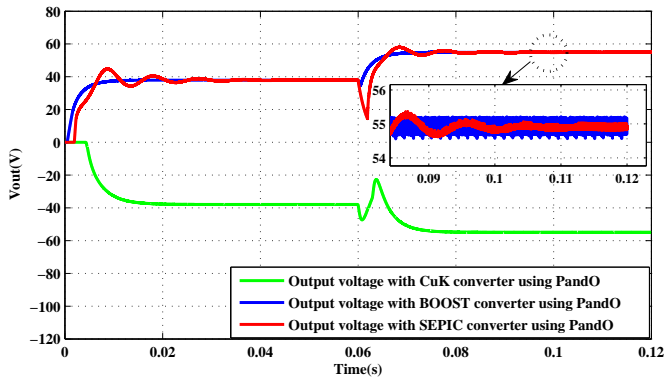


Fig. 12: Output voltage under variable irradiation using MPPT controller based on PandO algorithm.

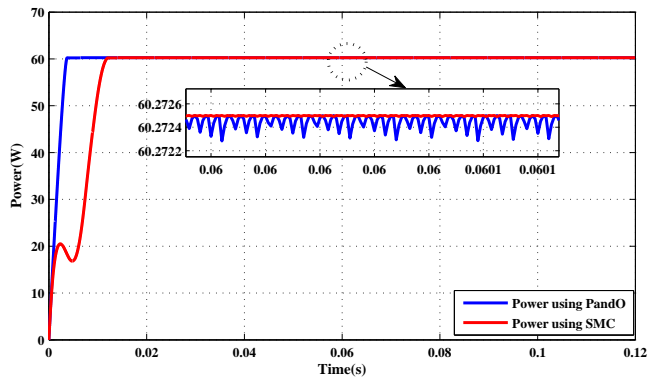


Fig. 13: Output power under load variation.

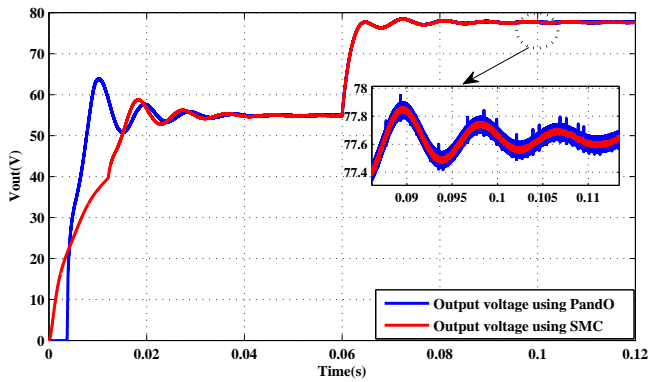


Fig. 14: Output voltage under load variation.

VI CONCLUSION

In this work, a complete study of PV systems integrating an MPPT controller was studied. The proposed PV system is composed of a PV generator, a boost converter and a resistive load. The maximum power point tracking techniques are used to deliver maximum possible power from the solar array. PandO with fixed perturb value is having tracking versus

oscillations tradeoff problem. MPPT controller based on sliding theory showed better performance with lower oscillation. Selection of one converter from the three depends on the system requirements and budget. For good quality of output power, SEPIC converter is favorable.

REFERENCES

- [1] I. Dullah, B. Mohi, A. Imtiaz, A.M. Liakot, *Renewable Energy Technologies for the Developing and Developed Countries Power Sector and Assessment of CO2 Mitigation Potential*, International Conference on Electrical and Computer Engineering ICECE '06, 2006.
- [2] S. Santonu, A. Venkataramana, *MW Resource Assessment Model for a Hybrid Energy Conversion System With Wind and Solar Resources*, IEEE Transactions on Sustainable Energy, vol. 2, no. 4, pp. 383-391, 2011.
- [3] A. Dolara, R. Faranda, S. Leva, *Energy Comparison of Seven MPPT Techniques for PV Systems*, Journal of Electromagnetic Analysis and Applications, vol. 1, no. 3, pp. 152-162, 2009.
- [4] E. Trishan, C.L. Patrick, *Comparison of Photovoltaic Array Maximum Power Point Tracking Techniques*, IEEE Transactions on Energy Conversion, vol. 22, no. 2, pp. 439-449, 2007.
- [5] N. Femia, G. Petrone, G. Spagnuolo, M. Vitell, *Increasing the efficiency of P&O MPPT by converter dynamic matching*, IEEE International Symposium on Industrial Electronics, vol. 2, no. 2, pp. 1017-1021, 2004.
- [6] D.S. Michael, R.S. Sanders, *Analysis and optimization of switched-capacitor DC-DC converters*, IEEE Transactions on Power Electronics, vol. 23, no. 2, pp. 841-851, 2008.
- [7] D.L. King, M.A. Quintana, J.A. Kratochvil, D.E. Ellibee, B.R. Hansen, *Photovoltaic module performance and durability following long-term field exposure*, Progress in Photovoltaics Research and Applications, vol. 8, no. 2, pp. 241-256, 2000.
- [8] S. Tarak, B. Mounir, G. Adel, M. Ahmed, *Matlab/simulink based modeling of photovoltaic cell*, International Journal of Renewable Energy Research (IJRER), vol. 2, no. 2, pp. 213-218, 2012.
- [9] E. Trishan, C. Patrick, *MComparison of photovoltaic array maximum power point tracking techniques*, IEEE Transactions on Energy Conversion EC, vol. 22, no. 2, pp. 439-449, 2012.
- [10] B. Andrzej, R.J. Patton, *Sliding mode control*, International Journal of Adaptive Control and Signal Processing, vol. 21, no. 8, pp. 635-637, 2007.
- [11] B. Domingo, G. Francesc, F. Enric, C. Javier, *Sliding-mode control design of a boost-buck switching converter for AC signal generation*, IEEE Transactions on Circuits and Systems I: Regular Papers, vol. 51, no. 8, pp. 1539-1551, 2004.
- [12] E. Mohammed, Z. Bashar, A. David, *Assessment of Perturb and Observe MPPT algorithm implementation techniques for PV pumping applications*, IEEE transactions on sustainable energy, vol. 3, no. 1, pp. 21-33, 2012.